

Quantum Adiabatic Brachistochrone

A. T. Rezakhani⁽¹⁾, W. -J. Kuo⁽¹⁾, A. Hamma⁽²⁾, D. A. Lidar⁽¹⁾, and P. Zanardi⁽¹⁾

⁽¹⁾*Departments of Chemistry, Electrical Engineering, and Physics,
and Center for Quantum Information Science & Technology,
University of Southern California, Los Angeles, CA 90089, USA and*

⁽²⁾*Perimeter Institute for Theoretical Physics, 31 Caroline St. N, N2L 2Y5, Waterloo ON, Canada*

We formulate a time-optimal approach to adiabatic quantum computation (AQC). A corresponding natural Riemannian metric is also derived, through which AQC can be understood as the problem of finding a geodesic on the manifold of control parameters. This geometrization of AQC is demonstrated through two examples, where we show that it leads to improved performance of AQC, and sheds light on the roles of entanglement and curvature of the control manifold in algorithmic performance.

PACS numbers: 03.67.Lx, 02.30.Xx, 02.30.Yy, 02.40.-k

Introduction.—Quantum computation is most commonly formulated in the language of the “circuit model” [1]. The problem of finding optimal quantum circuits – which minimize the number of gates used – was recently addressed in an elegant differential-geometric framework, wherein the minimum number of elementary gates for construction of a general n -qubit unitary U can be found by traversing the geodesic connecting the identity $\mathbb{1}$ to U over the $SU(2^n)$ manifold [2]. This approach is appealing since it allows for the application of powerful tools and techniques from variational calculus and differential geometry [3] to quantum computation. Adiabatic quantum computation (AQC) [4], on the other hand, is a very different approach which has recently attracted much attention due to its fundamental connection to quantum many-body systems, in particular to quantum phase transitions (QPTs) [5]. The basic strategy of AQC is to solve computational problems based on adiabatic evolution. A quantum system is prepared in the ground state of an initial Hamiltonian $H(0) = H_I$. The system is then driven to a final state, which – provided the evolution was adiabatic – is the ground state of a “problem Hamiltonian” $H(T) = H_P$. This final state corresponds to the solution of a hard problem, while a short time T corresponds to an efficient AQC strategy. Although AQC is equivalent in computational power to the circuit model [6], and relies on one of the oldest theorems of quantum theory – the adiabatic theorem [7] – it is still relatively unexplored. Specifically, an optimal strategy for AQC, akin to what has been done for the circuit model [2], has not yet been formulated.

In this work we reformulate AQC as a variational problem and develop a time-optimal strategy – a “quantum adiabatic brachistochrone” (QAB) – for quantum algorithms [8]. Specifically, we devise a variational time-optimal strategy for obtaining an interpolating Hamiltonian $H(t)$ between H_I and H_P , which gives rise to the shortest time T while guaranteeing that the actual final state (the solution to the corresponding Schrödinger equation), is close to the desired final ground state. We go further and show that the QAB can be recast in a natural differential-geometric framework. Specifically, we construct a Riemannian geometry, along with its corresponding metric, for the adiabatic evolution. We provide two examples which illustrate the advantage of this optimal approach.

Time-optimal AQC.— The adiabatic approximation, which underlies AQC, is often stated as follows [7]. Consider a system subjected to a time-dependent Hamiltonian $H(t)$, with a nondegenerate ground state $|\Phi_0(t)\rangle$ isolated by a nonvanishing gap $\Delta(t)$ from the first excited state $|\Phi_1(t)\rangle$. Let $D(t) \equiv |\langle \Phi_1(t) | \partial_t H(t) | \Phi_0(t) \rangle|$. Prepare the system in $|\psi(0)\rangle = |\Phi_0(0)\rangle$ and let it evolve according to the Schrödinger equation into the state $|\psi(T)\rangle$. Then, provided the time variation of the Hamiltonian is sufficiently slow, or T is sufficiently large, in that $\max_{t \in [0, T]} D(t) / \min_{t \in [0, T]} \Delta^2(t) \ll \epsilon$, the fidelity $F(T) \equiv |\langle \Phi_0(T) | \psi(T) \rangle|$ between the final ground state and the actual final state is high: $F \geq \sqrt{1 - \epsilon^2}$. However, it is well known that the latter condition is not always accurate [9], as recently verified experimentally [10]. Rigorous versions of the adiabatic approximation [11] typically involve $\|\partial_t H\|^2 / \Delta^3$ (with the norm being the maximum eigenvalue), or terms with different powers of $\|\partial_t H\|$ and Δ . As our approach is to use the adiabatic condition as a heuristic for finding optimal trajectories, the exact form of the adiabatic condition is in fact not essential: we shall judge success by the tradeoff between fidelity F and evolution time T . As we show below, this pragmatic approach also allows us to find time-optimal and geometric formulations of AQC.

The time-dependence of Hamiltonians usually comes from a set of control parameters $\mathbf{x}(t) = (x^1(t), \dots, x^M(t))$ – e.g., electric or magnetic fields, laser beams, or any other experimental “knob” – varying over a parameter manifold \mathcal{M} , whence $H = H[\mathbf{x}(t)]$. Varying the Hamiltonian for a given interval $t \in [t_0, t_1]$ then translates geometrically into moving along a control curve (or path) $\mathbf{x}(t)$ in \mathcal{M} . We can reparameterize \mathcal{M} via a dimensionless “natural parameter” $s(t)$ [3], with $s(0) = 0$ and $s(T) = 1$ (e.g., the normalized length), where $v(t) \equiv ds/dt > 0$ characterizes the speed by which we move along $\mathbf{x}[s(t)] \in \mathcal{M}$. To make the adiabatic dynamics locally compatible with the geometric structure of \mathcal{M} , we modify the adiabatic condition into the following local (i.e., instantaneous) form [12]:

$$\frac{v(s) \|\partial_s H(s)\|}{\Delta^2(s)} \ll \epsilon \quad \forall s \in [0, 1]. \quad (1)$$

Hereafter the norm is the Hilbert-Schmidt (or Frobenius)

norm, defined as $\|A\|_{\text{HS}} = \sqrt{\text{Tr}[A^\dagger A]}$. From the relation $T = \int_0^1 ds/v(s)$, we define the *adiabatic time-functional*

$$\mathcal{T}[\mathbf{x}(s)] = \int_0^1 \frac{ds}{v_{\text{ad}}[\dot{\mathbf{x}}(s), \mathbf{x}(s)]} \equiv \int_0^1 ds \mathcal{L}[\dot{\mathbf{x}}(s), \mathbf{x}(s)], \quad (2)$$

where $\dot{x} \equiv \partial_s x$. Inspired by the local adiabatic condition (1), we choose the instantaneous ‘‘adiabatic speed’’ via the *ansatz*

$$v_{\text{ad}}(s) \equiv \epsilon \Delta^2(s) / \|\partial_s H(s)\|, \quad (3)$$

and hence – using Einstein summation – the Lagrangian $\mathcal{L}[\dot{\mathbf{x}}(s), \mathbf{x}(s)] = \|\dot{x}^i \partial_i H[\mathbf{x}(s)]\| / \epsilon \Delta^2[\mathbf{x}(s)]$, where $\partial_i \equiv \partial / \partial x^i$. This ansatz is sensible, in that adiabaticity is hindered when the gap closes, while it is favored when the variation of the Hamiltonian is slow. To simplify the analysis, from now on, we take the Lagrangian to be $\mathcal{L}' = \mathcal{L}^2$; this corresponds to a reparameterization which leaves the length of the curve solving the Euler-Lagrange (EL) equations invariant [2, 3].

\mathcal{T} measures the time taken to traverse the curve $\mathbf{x}(s)$ from start to finish, subject to the local adiabatic condition (1). Our goal is to minimize this time and thus obtain the *time-optimal curve*, or set of time-dependent controls. This optimal curve is the QAB. From variational calculus, the optimal path $\mathbf{x}_{\text{QAB}}(s)$ should satisfy $\delta \mathcal{T}[\mathbf{x}(s)] / \delta \mathbf{x}(s) = 0$, which gives rise to the EL equations $d\dot{\mathbf{x}} \mathcal{L}'[\dot{\mathbf{x}}, \mathbf{x}] / ds = \partial_{\mathbf{x}} \mathcal{L}'[\dot{\mathbf{x}}, \mathbf{x}]$.

Some remarks regarding the QAB are in order. (i) The total real evolution time T (for a given fidelity F) is not necessarily the same as the time-functional \mathcal{T} . The correct interpretation is this: after finding the optimal path $\mathbf{x}_{\text{QAB}}(s)$ we solve the Schrödinger equation $i v_{\text{ad}} \partial_s |\psi\rangle = H |\psi\rangle$ with H and v_{ad} computed along the optimal path, to find $|\psi[\mathbf{x}_{\text{QAB}}(t)]\rangle$. The actual adiabatic error is then $\delta(T) \equiv \sqrt{1 - F_{\text{QAB}}(T)^2}$, where $F_{\text{QAB}}(T) \equiv |\langle \Phi_0(T) | \psi[\mathbf{x}_{\text{QAB}}(T)] \rangle|$, for a given T . With this interpretation it is safe to take $\epsilon \equiv 1$ in Eq. (3). Thus, we use \mathcal{T} as a guiding principle to obtain optimal paths; the actual adiabatic time and error should be calculated independently, as per the prescription above. (ii) Equation (1) and our corresponding choice of v_{ad} are by no means unique. They merely represent a convenient ansatz for our subsequent analysis, and it is quite possible that a better ansatz involving a different combination of $\|\partial_s H\|$ and Δ exists. (iii) The presence of Δ in \mathcal{L} implies that in order to apply our method, one needs to either find the gap exactly (which could be as hard as solving the problem itself), or restrict the interpolation to forms for which an explicit functional form for the gap can be obtained (e.g., in exactly- or almost-exactly-solvable models), or follow the scheme suggested to translate a quantum circuit model computation to an AQC (by which an interpolating Hamiltonian with an easily calculable gap is derived) [6], or estimate the gap by means of other methods (e.g., experimentally). (iv) The bottleneck of adiabatic algorithms is at the finite-size precursor of QPTs where the gap becomes small (and vanishes in the thermodynamic limit) [5]. The subtle point, however, is that due to the $\|\dot{x}^i \partial_i H\|$ factor in the numerator of \mathcal{L} , in principle, there is the possibility that one can (at least partially) suppress the vanishing gap and associated QPT [13]. The QAB

will inherently seek to identify such criticality-suppressing control strategies (relative to the specific adiabatic condition we have adopted here), if they exist. Indeed, we shall see this in our examples, below. (v) In general, not every choice for the norm $\|\cdot\|$ yields an analytic adiabatic velocity. Our choice of the Hilbert-Schmidt norm is made to ensure analyticity, and to simplify our calculations. We shall see below that this choice also enables a geometric treatment of the QAB problem. (vi) Modeling AQC usually necessitates a parameterization of the Hamiltonian. In general, though, this parameterization is not unique. For simplicity, consider the parametrization $H(\mathbf{x}) = \sum_i x^i \sigma_i$, where $\{\sigma_i\}_{i=1}^M$ are time-independent, noncommuting, linearly-independent Hermitian operators, chosen in accordance with the underlying structure of the optimization or physical problem in question. For example, in a multi-qubit system, $\{\sigma_i\}$ could represent (two-) local interactions in the form of the tensor product of Pauli matrices. It can be shown that in these ‘‘interaction coordinates,’’ the EL equations read:

$$\ddot{x}^k + \Gamma^k_{ij}(\mathbf{x}) \dot{x}^i \dot{x}^j = 0, \quad (4)$$

where

$$\Gamma^k_{ij} = 2 (C_{ij} C^{kl} \partial_l \Delta - \delta^k_i \partial_j \Delta - \delta^k_j \partial_i \Delta) / \Delta, \quad (5)$$

$C_{ij} \equiv (\mathbf{C})_{ij} = \text{Tr}[\sigma_i \sigma_j]$, and $C^{ij} = (\mathbf{C}^{-1})_{ij}$. (vii) Including various physical constraints into the variational description of AQC is natural through the Lagrange multiplier method.

Geometrization of AQC.—Motivated by the existence of a differential-geometric description for circuit optimization [2], and by the resemblance of Eq. (4) to a geodesic equation [3], we reformulate QAB in a differential-geometric language. This in turn endows AQC with a Riemannian manifold structure. An immediate advantage of this geometrization is that it equips AQC with the powerful techniques and tools of differential geometry, and shows that the problem of finding the QAB can be viewed as belonging to geometric control theory [14]. Furthermore, geometrization allows treating AQC and the circuit model in a universal geometric setting [2], which may suggest a natural alternative to Refs. [6] for proving the equivalence of AQC and the circuit model.

The transition from the EL equations to a geodesic equation is possible when one can write $\mathcal{L}'[\dot{\mathbf{x}}, \mathbf{x}] = g_{ij}(\mathbf{x}) \dot{x}^i \dot{x}^j$, where \mathbf{g} (with matrix elements g_{ij}) is a differentiable and invertible matrix [3]. From the definition of \mathcal{L} for the QAB, we then obtain

$$g_{ij}(\mathbf{x}) = \text{Tr}[\partial_i H(\mathbf{x}) \partial_j H(\mathbf{x})] / \Delta^4(\mathbf{x}), \quad (6)$$

which is the sought-after metric tensor. In interaction coordinates, for example, $\mathbf{g}(\mathbf{x}) = \mathbf{C} / \Delta^4(\mathbf{x})$, while it is represented differently in other coordinates [3].

In this framework, then, the QAB is equivalent to the geodesic over $(\mathcal{M}, \mathbf{g})$, and Eq. (4) is the geodesic equation, in which $\Gamma^k_{ij} = \frac{1}{2} g^{kl} (\partial_j g_{kl} + \partial_k g_{jl} - \partial_l g_{jk})$ are the connection coefficients [where $g^{ij} \equiv (\mathbf{g}^{-1})_{ij}$]. Since $g_{ij} \propto \Delta^{-4}$

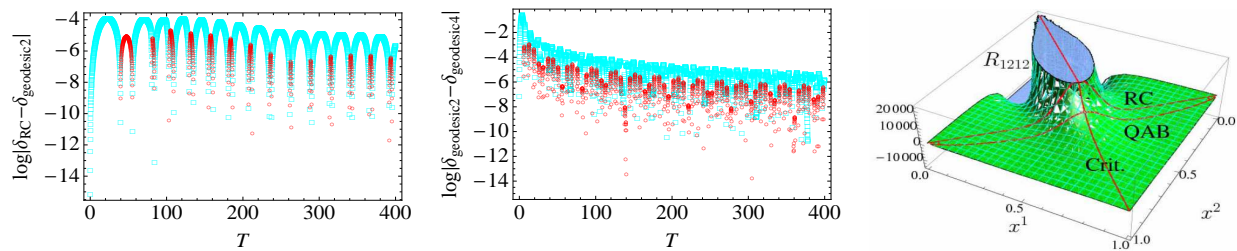


FIG. 1: (color online) Left: Final-time error $\delta(T)$ for the RC and 2-d geodesic paths for the Grover search problem, for $n = 6$ qubits. Squares (cyan) indicate where the 2-d geodesic path outperforms the RC path ($\delta_{\text{geodesic}} \leq \delta_{\text{RC}}$); circles (red) correspond to the opposite case. Oscillations are due to $\delta(T)$ itself being highly oscillatory, with an envelope $\propto 1/T$. Middle: $\delta(T)$ for the 2-d and 4-d geodesic paths, for $n = 1$. Cyan squares (red circles) indicate where the 4-d (2-d) geodesic path results in a smaller error. Right: Component $R_{1212}(x^1, x^2)$ of the curvature tensor for $n = 3$. The curves on the curvature surface show the critical line (vanishing gap as $n \rightarrow \infty$), the RC interpolation, and the 2-d geodesic (QAB). R_{1212} is the only independent component of the curvature tensor in this case [$R_{ijkl} = 2R_{1212}(g_{ik}g_{jl} - g_{il}g_{jk}) / \det g$].

(if the numerator does not contribute a power of Δ) we find $\Gamma \sim g^{-1}\partial g \sim \Delta^{-1}\partial\Delta$. Using standard expressions [3], one can calculate the Riemann curvature tensor \mathbf{R} from the connection coefficients and the metric tensor, yielding $\mathbf{R} \sim \partial^2 g + g\Gamma^2 \sim \Delta^{-6}$.

Examples.—We consider the following two-dimensional (2-d) interpolating Hamiltonian:

$$H(x^1(s), x^2(s)) = x^1(s)P_{\mathbf{a}}^\perp + x^2(s)P_{\mathbf{b}}^\perp, \quad (7)$$

where $P_{\mathbf{a}}^\perp = \mathbb{1} - |\mathbf{a}\rangle\langle\mathbf{a}|$ for the normalized vector $|\mathbf{a}\rangle \in \mathcal{H}$ with $\dim(\mathcal{H}) = N$ (similarly for $P_{\mathbf{b}}^\perp$), $\alpha_0 \equiv \langle\mathbf{a}|\mathbf{b}\rangle$ is a known function of N alone, and $x^1(0) = x^2(1) = 1$; $x^1(1) = x^2(0) = 0$. We can always find $|\mathbf{a}^\perp\rangle$ such that $|\mathbf{b}\rangle = \alpha_0|\mathbf{a}\rangle + \alpha_1|\mathbf{a}^\perp\rangle$, where $\langle\mathbf{a}|\mathbf{a}^\perp\rangle = 0$, and $\alpha_1 = \langle\mathbf{a}^\perp|\mathbf{b}\rangle$. Completing $\{|\mathbf{a}\rangle, |\mathbf{a}^\perp\rangle\}$ to a basis for \mathcal{H} we can easily diagonalize the Hamiltonian (7), and find that the gap between the ground state and the first excited state is $\Delta(x^1, x^2) = \sqrt{(x^1)^2 + (x^2)^2 + 2(2|\alpha_0|^2 - 1)x^1x^2}$. While the general 2-d problem requires a numerical solution, we find that if we impose a one-dimensional (1-d) constraint, i.e., $x(s) \equiv x^2(s) = 1 - x^1(s)$, then an analytical solution is possible:

$$x_{\text{QAB}}(s) = \frac{1}{2} - \frac{|\alpha_0|}{2\sqrt{1-|\alpha_0|^2}} \tan[(1-2s)\arccos|\alpha_0|]. \quad (8)$$

We now consider two illustrative problems which are special cases of the Hamiltonian (7).

Quantum search.—As a first illustration we revisit Grover’s unstructured search problem, which involves finding a marked object among N objects by repeated oracle queries [1, 15]. Grover’s quantum circuit model solution uses $O(\sqrt{N})$ queries, which is provably optimal, and a quadratic improvement over the best possible classical strategy. This problem was successfully recast in the AQC setting by Roland and Cerf (RC) [12], who considered the 1-d version of (7) with $x(s) \equiv x^2(s) = 1 - x^1(s)$, $|\mathbf{a}\rangle = \sum_{k=0}^{N-1} |k\rangle/\sqrt{N}$ (equal superposition), $|\mathbf{b}\rangle = |m\rangle$, and the fixed index $m \in \{0, \dots, N-1\}$ being the “marked item”. Thus $\alpha_0 = 1/\sqrt{N}$, with $N = 2^n$ the dimension of the Hilbert space of n qubits. It turns out that the optimal 1-d solution (8) coincides precisely with the

solution found by RC, who proved its optimality (in the sense of $O(\sqrt{N})$ scaling for a fixed error) without the use of variational optimization. We now extend the analysis by considering 2-d and 4-d parametrizations, which corresponds to finding optimal curves on 2-d and 4-d manifolds, respectively. The 2-d case is given by Eq. (7) and the discussion that follows it, with $|\mathbf{a}\rangle$ and $|\mathbf{b}\rangle$ as above. In the 4-d case, we first consider a general one-qubit Hamiltonian $H(x^1, x^2, x^3, x^4) = \frac{1}{\sqrt{2}}(x^1\mathbb{1} + x^2\sigma_x + x^3\sigma_y + x^4\sigma_z)$, and solve the corresponding geodesic (or QAB) differential equations. Next we recall that Grover’s search is effectively a 2-d problem (in the $\{|\mathbf{a}\rangle, |m\rangle\}$ basis). This enables us to use the 4-d setting for finding a Groverian geodesic path, with the proper boundary conditions corresponding to $|\mathbf{a}\rangle = \sqrt{(N-1)/N}|0\rangle + 1/\sqrt{N}|1\rangle$ and, for example, $|m\rangle = |1\rangle$. However, note that the parametrization of $H(x^1, x^2, x^3, x^4)$ above is not the most general 4-d parametrization when $n > 1$.

The 1-d RC analysis employed the local adiabatic condition (1) to recover the optimal scaling $T_{\text{opt}} \propto \sqrt{N}$, for $N \gg 1$. This might suggest that there is no room for further improvement, but we recall that in the AQC setting the fidelity is 1 only in the limit $T \rightarrow \infty$. Thus we compare the error $\delta(T)$ for the RC interpolation to the error obtained from the optimal 2-d interpolation. The result for $n = 6$ qubits is shown in Fig. 1 (left); results for other values of n are qualitatively similar, though the advantage of the optimal interpolation shrinks as n grows. *The optimal 2-d interpolation results in a smaller error for most values of T , a tendency that increases as T grows.* Conversely, for most values of the error δ the 2-d QAB requires a smaller time T than the RC curve. The middle panel shows the further improvement resulting from the 4-d interpolation. These results provide a rather striking demonstration of the power of our formalism, as due to its highly optimized nature, the Grover example is one where hardly any improvement was to be expected.

Figure 1 (right) depicts the RC and 2-d optimal curves over the curvature R_{1212} surface. Clearly, the optimal curve follows a path of lower curvature. This is confirmed in Fig. 2 (left), for different values of n . Figure 2 (right) depicts the amount of bipartite entanglement along the RC and 2-d opti-

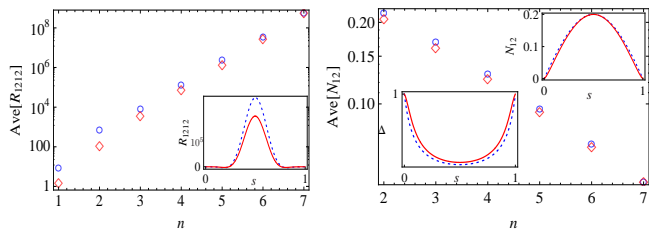


FIG. 2: (color online) Red diamonds or solid line (blue circles or dashed line) represent the 2-d QAB (RC) path. Left: Average curvature component R_{1212} vs n . Inset: instantaneous curvature for $n = 4$. Results for other values of n are qualitatively similar. Right: Same for negativity N_{12} [17] – between qubits 1 and 2. Inset: instantaneous gap (lower left) and negativity (upper right) for $n = 4$. Here, $\text{Ave}_\gamma[X] \equiv \int_\gamma X[\mathbf{x}(s)]ds / \int_\gamma ds$ for given path γ ; $X \in \{N_{12}, R_{1212}\}$ and $\gamma \in \{\text{RC}, \text{QAB}\}$. Note that same values of s (local time) do not necessarily indicate the same real (proper) time t for different paths.

mal paths. *In spite of its improved performance, there is less entanglement along the 2-d optimal path than along the RC path*, so that more entanglement does not always translate into higher algorithmic efficiency. We have verified (not shown) that the same picture emerges in terms of the entanglement entropy (or block entanglement) [16]. The explanation for this lower entanglement along the QAB is that it has a larger instantaneous gap than the RC path [Fig. 2 (right)]. Indeed, it has been shown that for Grover’s algorithm the entanglement entropy is small away from the finite-size precursor of the first-order QPT, but peaks near the critical point [5], and we have verified the same for the 2-d QAB. Finally, the reason that QAB follows a path with larger gap is that this is consistent with higher adiabaticity. By our previous scaling result $R \sim \Delta^{-6}$, it is also consistent with lower curvature.

Linear equations.—Solving linear equations of the type $A\mathbf{y} = \mathbf{a}$, where A is a given (Hermitian) $N \times N$ matrix and \mathbf{a} is a given vector, is a common problem. Recently a quantum algorithm was proposed in the circuit model that can obtain \mathbf{y} for well-conditioned, *sparse* matrices in a time scaling as $\text{polylog}(N)$ [18]. Here we consider the problem of finding $\mathbf{y} = A^{-1}\mathbf{a}$ as one of oracular *adiabatic state generation* [19]. To do so we let $|\mathbf{b}\rangle = A^{-1}|\mathbf{a}\rangle / \|A^{-1}|\mathbf{a}\rangle\|$. The formulation given above for the Hamiltonian (7) then applies. For concreteness we let $|\mathbf{a}\rangle = (1, \dots, 1)^T / \sqrt{N}$ and take A to be an $N \times N$ Toeplitz matrix whose first row and column are successive natural numbers, starting from 1. Toeplitz matrices have important applications in signal processing [20], and are not sparse. We then find $\alpha_0 = \sqrt{2/N}$ and hence can deduce immediately – by analogy to the Grover case, where $\alpha_0 = \sqrt{1/N}$ – that the optimal 1-d interpolation will give rise to a run-time T scaling as $O(\sqrt{N})$ for a fixed error. Moreover, 2-d and 4-d interpolations will further improve the error at fixed run-time. It is interesting to note that the most efficient known classical algorithm for inverting an $N \times N$ Toeplitz matrix requires $O(N \log^2 N)$ steps [20], though a direct comparison is not possible due to our oracular setting.

Conclusion and outlook.—We have presented a time-optimal, differential-geometric framework for AQC, and discussed its implications for the optimal design of adiabatic algorithms. The power of this new framework was illustrated via an example showing how the performance of an adiabatic algorithm can be improved by increasing the dimension of the control parameter space, and how geometrization sheds light on the role of entanglement and control manifold curvature in this enhanced performance. The method presented here is general and can in principle be used to optimize any adiabatic quantum algorithm for which the gap (or estimate thereof) is known. An important next step is to incorporate decoherence-mitigation strategies [21].

Acknowledgments.—Supported by the NSF under grants No. CCF-726439, PHY-802678, PHY-803304, and PHY-0803371, and by NSERC and MRI.

-
- [1] M. A. Nielsen and I. L. Chuang, *Quantum Computation and Quantum Information* (Cambridge University Press, Cambridge, UK, 2000).
 - [2] M. A. Nielsen *et al.*, *Science* **311**, 1133 (2006); M. A. Nielsen, *Quantum Inf. Comput.* **6**, 213 (2006).
 - [3] M. Nakahara, *Geometry, Topology and Physics* (Adam Hilger, New York, 1990).
 - [4] E. Farhi *et al.*, eprint quant-ph/0001106; E. Farhi *et al.*, *Science* **292**, 472 (2001).
 - [5] J. I. Latorre and R. Orús, *Phys. Rev. A* **69**, 062302 (2004); R. Schützhold and G. Schaller, *Phys. Rev. A* **74**, 060304 (2006).
 - [6] D. Aharonov *et al.*, *SIAM J. Comput.* **37**, 166 (2007); A. Mizel, D. A. Lidar, and M. Mitchell, *Phys. Rev. Lett.* **99**, 070502 (2007).
 - [7] A. Messiah, *Quantum Mechanics* (Dover Publication, New York, 1999).
 - [8] This QAB is essentially different from the brachistochrone derived from non-adiabatically constrained dynamics, as in: A. Carlini *et al.*, *Phys. Rev. Lett.* **96**, 060503 (2006).
 - [9] K. -P. Marzlin and B. C. Sanders, *Phys. Rev. Lett.* **93**, 160408 (2004); D. M. Tong *et al.*, *Phys. Rev. Lett.* **98**, 150402 (2007); R. MacKenzie *et al.*, *Phys. Rev. A* **76**, 044102 (2007); M. H. S. Amin, eprint arXiv:0810.4335.
 - [10] J. Du *et al.*, *Phys. Rev. Lett.* **101**, 060403 (2008).
 - [11] S. Jansen, M. -B. Ruskai, and R. Seiler, *J. Math. Phys.* **48**, 102111 (2007); D. A. Lidar, A. T. Rezakhani, and A. Hamma, eprint arXiv:0808.2697.
 - [12] J. Roland and N. J. Cerf, *Phys. Rev. A* **65**, 042308 (2002).
 - [13] G. Schaller, *Phys. Rev. A* **78**, 032328 (2008); M. B. Hastings, *J. Stat. Mech.* L01001 (2008).
 - [14] V. Jurdjevic, *Geometric Control Theory* (Cambridge University Press, Cambridge, UK, 1996).
 - [15] L. K. Grover, *Phys. Rev. Lett.* **79**, 4709 (1997).
 - [16] G. Vidal *et al.*, *Phys. Rev. Lett.* **90**, 227902 (2003).
 - [17] G. Vidal, R. F. Werner, *Phys. Rev. A* **65**, 032314 (2002).
 - [18] A. Harrow, A. Hassidim, and S. Lloyd, eprint arXiv:0811.3171.
 - [19] D. Aharonov and A. Ta-Shma, *SIAM J. Comput.* **37**, 47 (2007).
 - [20] G. S. Ammar and W. B. Gragg, *SIAM J. Matrix Anal. Appl.* **9**, 61 (1988).
 - [21] S. P. Jordan, E. Farhi, and P. W. Shor, *Phys. Rev. A* **74**, 052322 (2006); D. A. Lidar, *Phys. Rev. Lett.* **100**, 160506 (2008).